mental Section, are shown in Figure 4 and are more revealing. PVF_2 (Figure 4A) displays a main relaxation (β) at −35 °C as well as the broad α relaxation at ≃90 °C.[13,16,19] PVF (Figure 4B) displays a main relaxation at 70 °C in addition to another very broad relaxation at −15 °C in good agreement with data presented in the literature.[13,19] The pattern of the 50/50 wt % blend (Figure 4C) displays a well-defined relaxation at −35 °C and a very broad relaxation between 60 and 95 °C. The patterns shown in Figure 4 taken as a whole indicate that the PVF_2 and PVF homopolymers used here are also immiscible in the amorphous phase.

Acknowledgment. We thank Prof. G. Allegra of the University of Milan and Prof. P. Corradini of the University of Naples for useful discussions. This work was supported by AFOSR 84-0101. G.G. thanks the Consiglio Nazionale delle Ricerche for support.

Registry No. PVF_2 (homopolymer), 24937-79-9; PVF (homopolymer), 24981-14-4.

References and Notes

(1) Natta, G.; Allegra, G.; Bassi, I. W.; Sianesi, D.; Caporiccio, G.; Torti, E. *J. Polym. Sci., Part A* **1965**, *3*, 4263.
(2) Doll, W. W.; Lando, J. B. *J. Macromol. Sci., Phys.* **1970**, *B4*, 897.
(3) Bychkov, R. A.; Gal'perin, Ye. L.; Konkin, A. A. *Vysokomol. Soedin., Ser. A.* **1971**, *13*, 1156.
(4) Hasegawa, R.; Takahashi, Y.; Chatani, Y.; Tadokoro, H. *Polym. J. (Tokyo)* **1972**, *3*, 600.
(5) Weinhold, S.; Litt, M. H.; Lando, J. B. *J. Polym. Sci., Polym. Lett. Ed.* **1979**, *17*, 585.
(6) Natta, G.; Bassi, I. W.; Allegra, G. *Acad. Naz. Lincei, Rend. Sci. Fis. Mat. Nat.* **1961**, *31*, 350.
(7) Lee, H.; Salomon, R. E.; Labes, M. M. *Macromolecules* **1978**, *11*, 171.
(8) Godovskii, Yu K.; Zharikova, Z. F.; Malinskii, Yu M. *Vysokomol. Soedin Ser. A* **1981**, *23*, 133.
(9) Olabisi, O.; Robeson, L. M.; Shaw, M. T. *Polymer–Polymer Misicibility*; Academic: New York, 1979; Chapter 5.
(10) Wunderlich, B. *Macromolecular Physics*; Academic: New York, 1976; Vol. 1, Chapter II; 1980; Vol. 3, Chapter VIII.
(11) Lovinger, A. J. "Poly(vinylidene fluoride)" In *Developments in Crystalline Polymers-1*; Basset, D. C., Ed.; Applied Science: London and New Jersey, 1982; Chapter 5.
(12) Zverev, M. P.; Polovikhina, L. A.; Barash, A. N.; Mal'kova, L. P.; Litovchenko, G. D. *Vysokomol. Soedin., Ser. A* **1974**, *16*, 1813.
(13) Görlitz, M.; Minke, R.; Trautvetter, W.; Weisgerber, G. *Angew. Makromol. Chem.* **1973**, *29/30*, 137.
(14) Kalfoglou, N. K.; Williams, H. L. *J. Appl. Polym. Sci.* **1973**, *17*, 3367.
(15) Furukawa, T.; Aiba, J.; Fukada, E. *J. Appl. Phys.* **1979**, *50*, 3615.
(16) Lovinger, A. J.; Wang, T. A. *Polymer* **1979**, *20*, 725.
(17) Gal'perin, Ye. L.; Kosmynin, B. P.; Smirnov, V. K. *Vysokomol. Soedin., Ser. A* **1970**, *12*, 1880.
(18) Gal'perin, Ye. L.; Kosmynin, B. P.; Smirnov, V. K. *Vysokomol. Soedin., Ser. B.* **1970**, *12*, 555.
(19) Enns, J. B.; Simha, R. *J. Macromol. Sci., Phys.* **1977**, *B13*, 11.

Phase Behavior of Amorphous Binary Mixtures of Perdeuterated and Normal 1,4-Polybutadienes

F. S. Bates* and S. B. Dierker

AT&T Bell Laboratories, Murray Hill, New Jersey 07974

G. D. Wignall

National Center for Small Angle Scattering Research, Oak Ridge National Laboratory, Oak Ridge, Tennessee 37831. *Received February 5, 1986*

ABSTRACT: A series of amorphous binary mixtures of normal and perdeuterated 1,4-polybutadienes has been examined by small-angle neutron scattering (SANS). Contrary to the generally held assumption that isotopic polymer mixtures form ideal solutions, we conclusively demonstrate that these mixtures are characterized by an upper critical solution temperature (UCST). This isotope effect derives from a small, measurable difference in segment volume between normal and perdeuterated species. Above the UCST, the SANS results are quantitatively predicted by the mean-field theory of de Gennes for homogeneous binary polymer mixtures. Increasing the degree of polymerization raises the critical temperature, resulting in phase separation. Owing to the combined effects of the close proximity to the consolute point and a small segment–segment interaction parameter ($\chi \simeq 10^{-3}$), the phase-separated mixtures exhibit extensive interfacial mixing; Porod analysis of the SANS results reveals an average interfacial thickness of $\langle D \rangle$ = 250 Å. Overall, these findings demonstrate that normal and perdeuterated amorphous polymers represent a new class of materials with which to study polymer–polymer phase behavior.

Introduction

The introduction of coherent elastic small-angle neutron scattering (SANS) to the study of macromolecules over a decade ago[1,2] represents one of the most significant experimental developments in the relatively brief history of polymer science. A recent review article[3] outlines the broad range of applications of this technique to the investigation of solution and bulk properties of polymers and polymer mixtures. What most distinguishes SANS from small-angle X-ray scattering (SAXS)[4] is the unique ability to selectively introduce a scattering length density difference (contrast) between or within molecules by substituting deuterium for hydrogen. In general, it has been assumed that this method of isotope labeling produces no other perceptable chemical or physical effects in polymer melts.

Isotope substitution leads to numerous alterations in the physical and chemical properties of condensed matter. Perhaps the most universally recognized thermodynamic effects are the differences in melting and boiling temperatures exhibited by isotopically different molecules (or atoms). For example, heavy water boils at 101.4 °C and melts at 3.8 °C,[5] deuterium ($^2H_2$) melts and boils at 4.5 and

0024-9297/86/2219-1938$01.50/0

3.2 °C, respectively, greater than hydrogen ($^1H_2$),[5] and perdeuteriobenzene melts and boils at 6.8 and 79.1 °C compared with the corresponding temperatures of 5.5 and 80.1 °C for normal (hydrogenous) benzene. Such thermodynamic differences also occur in high polymers.

Apparently Stehling et al.[6] first documented the fact that perdeuteriopolyethylene exhibits a melting temperature approximately 6 °C greater than that of normal polyethylene, suggesting that mixtures of these molecules could segregate upon crystallization; this was subsequently verified by researchers studying polyethylene crystallization by SANS.[7] Strazielle and Benoit[8] demonstrated that the Θ temperature of polystyrene in cyclohexane varied by about 4 °C depending upon the isotopic constitution of either the solvent or polymer. And recently, studies of phase transitions in polymer–polymer mixtures revealed that the consolute temperature varies markedly upon substituting deuterated for normal polymer;[9,10] Yang et al.[10] report that the lower critical solution temperature (LCST) of polystyrene–poly(vinyl methyl ether) mixtures increases by as much as 40 °C when normal polystyrene is replaced by the perdeuterated equivalent.

In each of the examples cited, substitution of deuterium for hydrogen has been observed to influence a phase transition. These effects are readily appreciated since phase transitions occur when entropic and energetic contributions to the free energy of a system *exactly* satisfy those criteria embodied in classical thermodynamics. There is nother particularly striking about the fact that subtle variations in the physical properties of a molecule, such as doubling the mass of all of the hydrogen atoms, produces minor variations in phase transition temperatures. That the critical temperature for a binary polymer mixture is influenced by isotope substitution is not surprising; this effect has also been observed in mixtures of small molecules.[11] Unfortunately, these isotope-related shifts in phase transition points are generally of no utility, serving merely to complicate contrast enhancement techniques. On the other hand, isotope-induced phase transitions in binary liquid mixtures of otherwise chemically identical components constitutes a fundamentally important and useful phenomenon. Until the present, however, studies of such effects have been exclusively restricted to mixtures of ^3He and ^4He.[12]

In the present paper we report in detail on the SANS-determined phase behavior of binary liquid mixtures of perdeuterated and normal 1,4-polybutadienes; the initial findings of this research have been published elsewhere.[13] These results provide the first example of an isotope-induced phase transition in amorphous mixtures of otherwise chemically identical polymers, clearly demonstrating that such mixtures do not form ideal solutions as generally assumed.

Experimental Section

Normal (protonated) and perdeuterated 1,4-polybutadienes were prepared by anionic polymerization of butadiene at 50 °C in benzene using *n*-butyllithium ($\simeq 1 \times 10^{-3}$ M) as the initiator. The initiation rate was selectively increased by the addition of a 3:1 ratio of anisole relative to lithium. Polymerizations were terminated with methanol. Butadiene monomers were obtained from Matheson (instrument purity) and Merck, Sharp and Dohme, LTD. (98.8 atom % deuterium labeled), and purified using standard techniques. The polymers were recovered by precipitation in methanol followed by vacuum drying and storage under a highly purified argon atmosphere. The polymers were characterized for number-average degree of polymerization N_N and polydispersity N_W/N_N by membrane osmometry and high-pressure size-exclusion chromatography (HPSEC); these results are summarized in Table I. Polybutadiene microstructure was determined by ^{13}C NMR spectroscopy using a 15% (w/v) solution of sample B5 in deuteriochloroform. Independent analysis of the olefinic and aliphatic regions of the ^{13}C NMR spectrum, based on the chemical shift assignments of Clague et al.,[14] confirmed a microstructure characteristic of lithium-catalyzed polybutadiene: 53% trans, 36% cis, and 11% vinyl. This microstructure agrees within experimental error with that reported by Atkin et al.[9] for perdeuterated polybutadiene prepared under the same conditions. These samples are referred to as 1,4-polybutadiene. Further details concerning the synthesis and characterization of polybutadienes can be found in a previous publication.[15]

Table I
1,4-Polybutadiene[a] Molecular Characterization

polymer	isotope	$N_n \times 10^{-3}$ [b]	N_w/N_n [c]
B2	^2H	4.2	1.10
B3	^1H	3.8	1.12
B5	^1H	0.91	1.05

[a] 53% trans, 36% cis, 11% vinyl as measured by ^{13}C NMR. [b] Number-average degree of polymerization as determined by membrane osmometry. [c] Polydispersity index as determined by HPSEC.

The density of samples B2 ($\rho_1 = 0.9962$ g/cm^3) and B3 ($\rho_2 = 0.8941$ g/cm^3) was measured at room temperature by a water displacement technique[16] using approximately 1.5 g of each polymer. These measurements were further substantiated by density gradient column measurements ($\rho_1 = 0.996$, $\rho_2 = 0.894$). Of particular significance to the present work is the relative specific volume difference $\Delta V/V$ between perdeuterated and normal 1,4-polybutadiene (see Discussion), where $\Delta V = V_2 - V_1$. On the basis of a mass correction corresponding to 98.8 atom % deuterium substitution (see above), $\Delta V/V = 4.1 \times 10^{-3}$. Within experimental error, this value agrees with that measured for various aliphatic and aromatic liquid hydrocarbons.[17]

Small-angle neutron scattering (SANS) data were obtained over the range of scattering wavevectors $3.5 \times 10^{-3} < q < 0.2$ Å^{-1} on the 30-m instrument located at the National Center for Small Angle Scattering Research, Oak Ridge National Laboratory, employing 4.75-Å-wavelength neutrons characterized by a wavelength distribution of $\Delta\lambda/\lambda \cong 0.05$. Scattered neutrons were counted on a two-dimensional position-sensitive area detector and corrected for background and cell scattering, detector sensitivity, sample thickness, and transmission. All scattering patterns were found to be azimuthally isotropic and were therefore azimuthally averaged to one-dimensional form. The SANS instrument was calibrated in units of absolute differential scattering cross-section per unit solid angle per unit volume of sample (cm^{-1}, ±5%) with an irradiated aluminum secondary standard (A1-4), which was independently calibrated against the incoherent scattering from water and vanadium, and the coherent scattering from a well-characterized polystyrene sample.

Scattering sample temperature was controlled (±0.1 °C) via a circulating temperature bath. Successive data sets were collected following a temperature change until the scattering intensity became time invariant, at which point the reported data were collected.

SANS specimens were prepared by dissolution of polymer B2 with either B3 or B5 in cyclohexane, followed by solvent evaporation and drying under vacuum ($\simeq 10^{-3}$ torr). Aliquots of dry polymer mixture were squeezed between quartz windows; this procedure was conducted under vacuum (10^{-4} torr) in order to avoid any entrapment of bubbles. Homopolymer scattering specimens were also prepared from samples B2 and B3 with the same procedures. SANS specimens were stored under a high-purity argon atmosphere prior to measurement.

Speciments subjected to neutron scattering measurements were also examined by light scattering. The angular dependence of the light scattering intensity was measured with an automated laser light scattering goniometer using the 5145-Å argon laser line. The scattered intensity was strongly modulated by a static speckle pattern due to the coherence of the incident laser beam and essentially static refractive index inhomogeneities in the sample. This modulation was removed by destroying the laser beam coherence with a rotating ground glass phase scrambler while still maintaining a well-collimated beam. With this technique, the

Table II
Structural Characteristics of Phase-Separated Mixtures

mixture	Φ^a	$\Phi_1{}^b$	D,[c] Å	L_P,[d] μm	L_{LS},[e] μm
B2B3(0.38)	0.384	0.13 ± 0.02	270	0.30	5.6
B2B3(0.29)	0.294	0.13 ± 0.02	240	0.28	4.6
B2B3(0.20)	0.200	0.13 ± 0.02	225	0.37	
B2B3(0.10)	0.100	0.07 ± 0.01		30–40	
B2B3(0.05)	0.050	0.008 ± 0.001	250	36	

[a] Stoichiometric volume fraction of polymer B2. [b] Volume fraction of polymer B2 as determined by SANS. [c] Interfacial thickness determined by SANS. [d] Porod heterogeneity length determined by SANS. [e] Heterogeneity length determined by light scattering.

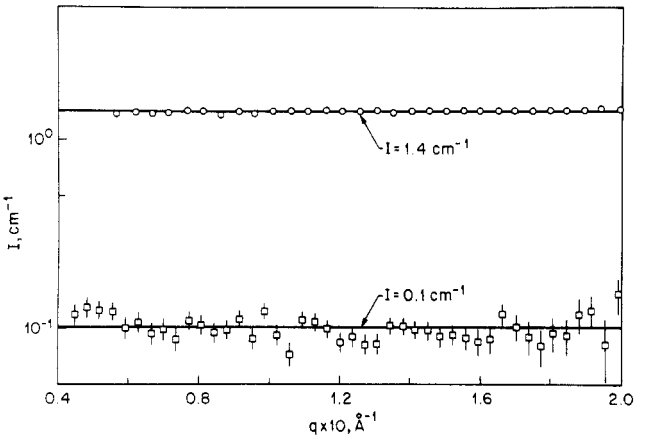

Figure 1. Small-angle scattering of neutrons from normal (○) and perdeuterated (□) 1,4-polybutadiene homopolymer at 296 K. The q-independent intensity derives predominantly from incoherent scattering events. SANS data obtained from mixtures of such polymers have been corrected for incoherent scattering by subtracting a weighted sum of these pure component intensities.

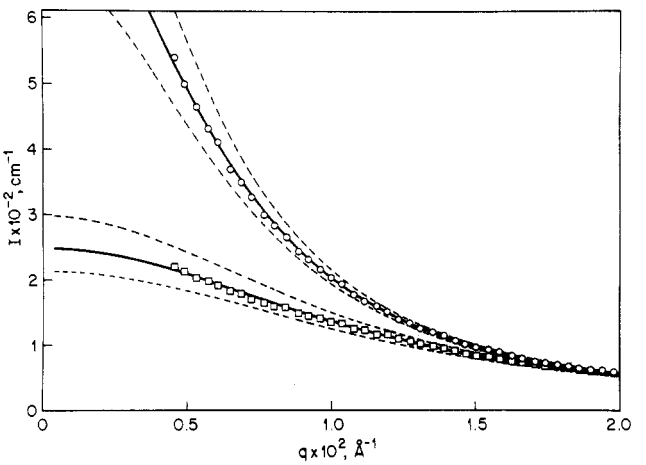

Figure 2. Coherent SANS results from mixtures B2B5(0.31) (○) and B2B5(0.65) (□) obtained at 296 K. The solid curves are the predicted scattering profile for homogeneous (single-phase) mixtures (eq 1 and 7) with $\chi = 8.7 \times 10^{-4}$. Sensitivity of the predicted scattering intensity to variations in χ is indicated by the upper ($\pm 5 \times 10^{-5}$) and lower ($\pm 1.3 \times 10^{-4}$) sets of dashed curves.

angular dependence of the scattering intensity was quite smooth and yet the angular resolution was still better than 1.5°. The scattering angle was corrected for the refractive indices of polybutadiene and quartz. The range of momentum transfers for the light scattering measurements reported corresponds to an external angular range of 2°–15°.

Results and Analysis

We have investigated the neutron and light scattering characteristics of two sets of binary mixtures prepared by blending sample B2 with samples B3 and B5 (Table I). These mixtures are referred to as B2B3(Φ) and B2B5(Φ)

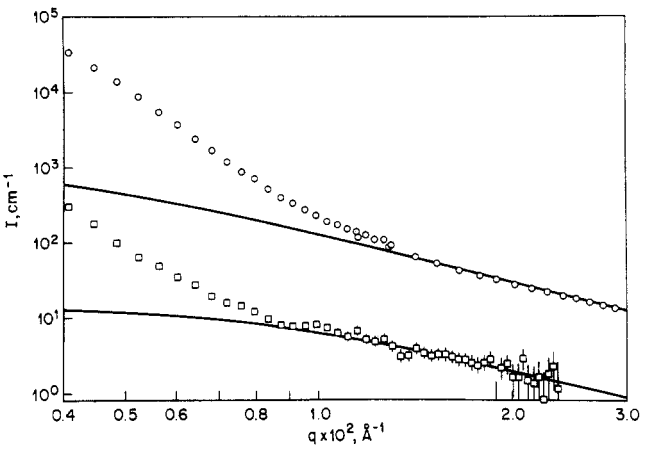

Figure 3. Coherent SANS results from two representative phase-separated mixtures, samples B2B3(0.29) (○) and B2B3(0.05) (□). The curves correspond to the estimated single-chain scattering contribution to the total scattering intensity. SANS intensity in excess of the curves ($q \lesssim 0.01$) derives from interfacial (Porod) scattering.

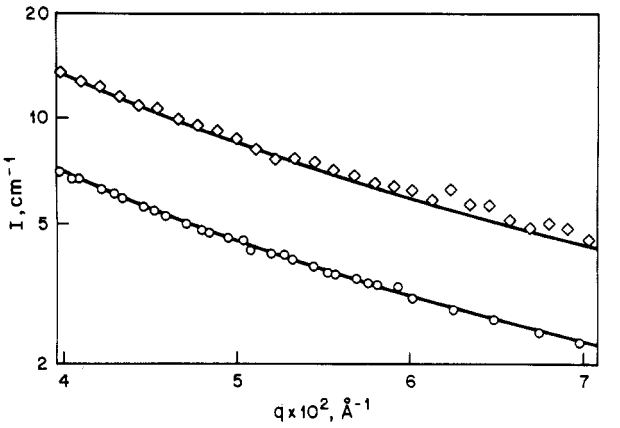

Figure 4. Representative coherent SANS results ($R_g q \gg 1$) for a homogeneous and a phase-separated mixture, samples B2B5-(0.31) (◇) and B2B3(0.29) (○), respectively. The upper curve has been calculated (eq 4 and 7) based solely on experimentally determined parameters. The lower curve has been fit to the data, providing an estimate of domain composition.

in Table II, where Φ denotes the volume fraction of the perdeuterated component.

The incoherent contribution to the measured neutron scattering intensities has been approximated based on a linear combination of the q-independent incoherent scattering intensities obtained from samples B2 and B3, as illustrated in Figure 1, where $q = 4\pi\lambda^{-1} \sin(\theta/2)$ represents the scattering wavevector. Although this linear incoherent scattering correction is not rigorously correct,[3] the errors associated with its application are negligible over the reported range of intensities and wavevectors. Coherent scattering intensities were obtained by subtracting the estimated incoherent intensity from the measured scattering intensity. The low q coherent scattering results

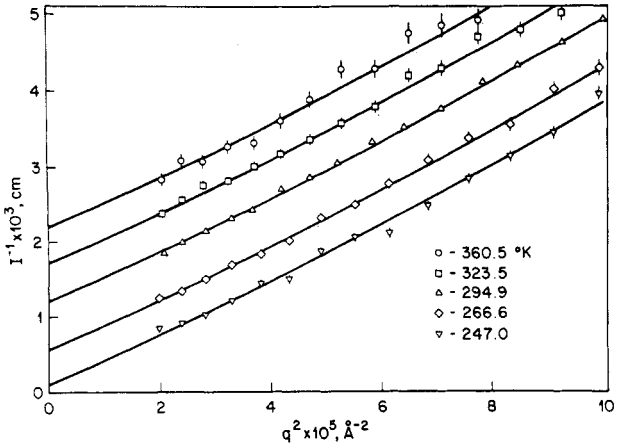

Figure 5. Temperature dependence of the critical scattering from (homogeneous) sample B2B5(0.31). The curves have been obtained based on the homogeneous binary mixture correlation function (eq 1) by adjusting the segment–segment interaction parameter χ.

for sample sets B2B5 and B2B3, measured at room temperature (296 K), are presented in Figures 2 and 3, respectively. Higher wavevector results are given in Figure 4 for two representative samples, B2B5(0.31) and B2B3-(0.29). Sample B2B5(0.31) was further examined during a series of heating and cooling sequences, covering a temperature range from 247 to 363 K. SANS results obtained at several representative temperatures are presented in Ornstein–Zernike form (reciprocal intensity vs. q^2) in Figure 5.

Mixtures constituting the B2B3 sample set were found to scatter visible light in considerable excess of that characterizing homopolybutadiene. This was particularly evident in samples B2B3(0.38), B2B3(0.29), and B2B3-(0.20), which were observed by the unaided eye to be slightly cloudy. The light scattering results obtained from these three samples are presented in Figure 6; the corresponding data from B2B3(0.10) and B2B3(0.05) qualitatively resemble the featureless results from B2B3(0.20) and have thus been omitted. The angular dependence of the light scattering intensity for samples B2B5(0.31) and B2B5(0.65) was indistinguishable from that for polybutadiene homopolymer at 296 K.

We have found the small-angle neutron scattering results from sample sets B2B5 and B2B3 to be qualitatively very different, deriving from differences in phase state, the former being homogeneous (single phase) and the later phase separated (two phase). In order to facilitate data interpretation, these two sets of SANS results are treated separately. A unifying analysis of these findings is presented in the Discussion.

Homogeneous Mixtures (Samples B2B5). de Gennes[18] has calculated the scattering structure factor $S(q)$ for homogeneous binary polymer blends based on the mean-field random-phase approximation (RPA)

$$S^{-1}(q) = [N_1\Phi g_D(R_{g1},q)]^{-1} + [N_2(1-\Phi)g_D(R_{g2},q)]^{-1} - 2\chi \quad (1)$$

in which g_D is the Debye function

$$g_D(R_g,q) = 2\left[R_g^2q^2 + e^{-R_g^2q^2} - 1\right]/R_g^4q^4 \quad (2)$$

and R_g is the radius of gyration of an ideal (Gaussian) coil

$$R_g^2 = a^2N/6 \quad (3)$$

where N is the weight-average degree of polymerization,[18] a is the (segment) length dictated by N and Gaussian

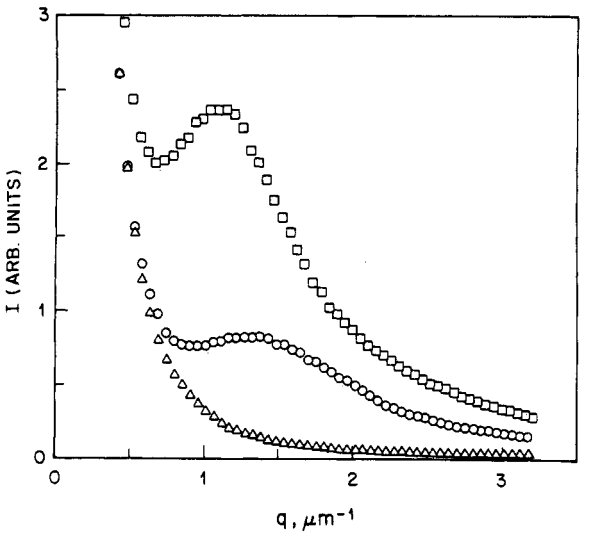

Figure 6. Light scattering results from phase-separated mixtures B2B3(0.38) (□), B2B3(0.29) (○), and B2B3(0.20) (△).

statistics, χ is the Flory segment–segment interaction parameter (see eq 14), and $\Phi = \Phi_1 = 1 - \Phi_2$ (incompressibility assumption).

In the limit $R_gq \gg 1$, eq 1 reduces to

$$S(q) = 12\Phi(1-\Phi)/a^2q^2 \qquad (R_gq \gg 1) \quad (4)$$

while in the limit $R_gq \ll 1$, $S(q)$ can be represented in Ornstein–Zernike form[18]

$$S(q) = \tfrac{1}{2}(\chi_S - \chi)^{-1}/(1 + q^2\xi^2) \qquad (R_gq \ll 1) \quad (5)$$

$$\xi = (a/6)[\Phi(1-\Phi)(\chi_S - \chi)]^{-1/2} \quad (6)$$

where ξ and χ_S refer to the composition fluctuation correlation length and stability limit (see eq 15), respectively.

We have analyzed the neutron scattering data from samples B2B5(0.31) and B2B5(0.65) based on eq 1. The scattering intensity is given by

$$I(q) = V^{-1}(b_H - b_D)^2S(q) \quad (7)$$

in which $V = 1.00 \times 10^{-22}$ cm^3 is the polymer segment volume, (see Experimental Section) and $b_H = 0.413 \times 10^{-12}$ cm and $b_D = 6.659 \times 10^{-12}$ cm are the coherent scattering lengths of the normal and perdeuterated segments.[19] The statistical (segment) length a has been estimated from literature data[20] to be $a = 6.9$ Å. As indicated by the upper solid curve in Figure 4, eq 4 quantitatively accounts for the high q SANS data based solely on experimentally determined parameters. This confirms the homogeneous (single-phase) state of this sample. At lower scattering wavevectors, the structure factor $S(q)$ becomes sensitive to segment–segment interactions. Therefore, the results presented in Figure 2 have been modeled with eq 1, using χ as a fitting parameter; all other parameters including scattering intensity have been independently determined. Both sets of SANS data are quantitatively predicted by the theoretical scattering function as indicated by the solid curves in Figure 2, yielding a single interaction parameter $\chi = 8.7 \times 10^{-4}$; the dashed curves illustrate the sensitivity of the prediction to variations in χ.

The temperature dependence of χ has been determined by fitting eq 1 to the $q < 0.01$ Å^{-1} data obtained during the heating and cooling of sample B2B5(0.31) as illustrated by the solid curves in Figure 5. It is important to emphasize that the Ornstein–Zernike form of $S(q)$ given by eq 5 is *not* applicable to these results since the data have been collected over the range $R_gq \geq 0.8$ based on the radius of gyration of polymer B2; this point is evidenced by the

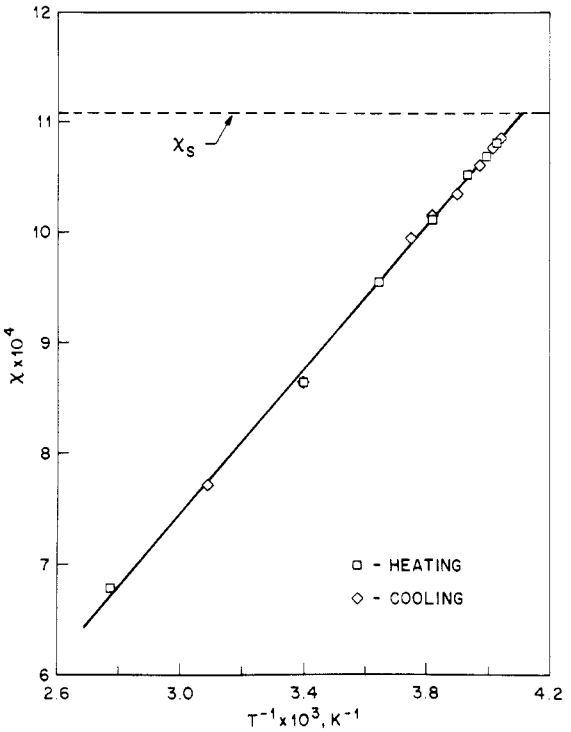

Figure 7. Temperature dependence of the segment–segment interaction parameter obtained by fitting the homogeneous binary mixture correlation function to the SANS results (Figure 5). χ_s corresponds to the calculated (eq 15) limit of single-phase stability.

curvature in the calculated curves in Figure 5. As presented in Figure 7, χ has thus been determined to be inversely related to temperature, $\chi = 0.326(\pm 0.004)T^{-1} - 2.3(\pm 1.7) \times 10^{-4}$, independent of sample thermal history. The error associated with the constant term in $\chi(T)$ derives from the uncertainty in the degrees of polymerization and SANS intensity calibration.

Phase-Separated Mixtures (Samples B2B3). For two-phase binary polymer mixtures eq 4 is replaced by (neglecting interfacial mixing, see below)

$$S(q) = \{\Phi'[\Phi_1'(1-\Phi_1')] + \Phi''[\Phi_1''(1-\Phi_1'')]\}/a^2q^2 \qquad (R_g q \gg 1) \tag{8}$$

where Φ' ($=1-\Phi''$) and Φ_1' refer to the volume fraction of phase (′) and component 1 in phase (′) respectively. Hence, for $R_g q \gg 1$ phase separation reduces the magnitude, without affecting the form, of the scattering intensity relative to the homogeneous state. This point is demonstrated by the SANS data from sample B2B3(0.29) in Figure 4. In the symmetrical case ($N_1 = N_2$) $\Phi_1'' = 1 - \Phi_1' = \Phi_1$,[21] whereby the absolute scattering intensity affords a direct measure of phase composition. On the basis of the near equivalence in polymerization indices of polymers B2 and B3 (Table I), we have thus determined the phase composition Φ_1 of the B2B3 mixtures. These results are listed in Table II. All the B2B3 samples are characterized by a measured phase composition Φ_1 significantly less than the composition Φ corresponding to the mixing stoichiometry, indicating that these mixtures have phase separated.

The effects of phase separation on the SANS measurements are also dramatically manifested in the low q region of the scattering results found in Figure 3. At wavevectors $q \lesssim 0.01$ Å^{-1} the scattering intensity exhibits positive deviations from Porod's law, indicative of an isotropic two-phase structure characterized by diffuse interphases. As first demonstrated by Ruland,[22] the actual interfacial profile can be modeled as the convolution of an ideal (step) interface with an appropriate smoothing function. The measured scattering intensity is thus given by

$$I(q) = 2\pi(s/v)(\rho_i - \rho_j)^2 q^{-4} h^2(q) \tag{9}$$

where $h(q)$ is the Fourier transform of the interfacial smoothing function, ρ_i is the average scattering length density of domain i, and s/v is the interfacial area per unit volume. For ideal periodic structures[4]

$$(s/v) \cong 2/L_P \tag{10}$$

where L_P represents the Porod heterogeneity length.

Helfand[23] and Leibler[24] have theoretically shown that the composition profile of the interfacial region of coexisting polymer phases consisting of symmetric components ($N_1 = N_2$; $a_1 = a_2$) is given by the classical[25] mean field profile

$$\Phi(x) = \tfrac{1}{2}[1 + (1 - 2\Phi_1)\tanh(x/D)] \tag{11}$$

in which Φ_1 is the domain composition ($x \to -\infty$) and D is a measure of the interfacial thickness. From this relationship, the attenuation function $h(q)$ can be determined to be[26]

$$h(q) = \int_{-\infty}^{\infty} dx\, e^{-iqx}\, d\Phi(x)/dx \tag{12}$$

$$h(q) = \frac{(1 - 2\Phi_1)(\pi Dq/2)}{\sinh(\pi Dq/2)} \tag{13}$$

The Porod intensity can be obtained by subtracting the coherent scattering associated with the mixed regions within each domain from the total coherent scattering intensity. In the limit $L_p \gg D$ (Table II), this contribution to the total intensity can be accurately estimated by extrapolation of eq 1, based on the composition determined for $R_g q \gg 1$ and $Dq \gg 1$. These corrections, indicated by the solid lines in Figure 3, have been determined by using the compositions Φ_1 listed in Table II, and $\chi = 8.7 \times 10^{-4}$ as determined independently in the homogeneous state (Figures 2 and 7) at room temperature. Porod plots (ln $(q^4 I)$ vs. q^2) of the corrected data are presented in Figure 8. We have determined the interfacial thickness D and two-phase heterogeneity (Porod) length L_P by fitting eq 9 and 13 to these data as illustrated by the solid lines in Figure 8; these results are summarized in Table I. With the exception of sample B2B3(0.10), all the mixtures examined are characterized by approximately the same interfacial thickness, $\langle D \rangle = 250$ Å. Owing to the relatively large values of both Φ_1 and L_P, the uncertainty associated with the single-chain scattering correction renders the interfacial thickness measurement for sample B2B3(0.10) statistically meaningless; it has therefore been omitted from Table II. Also listed in Table II is the heterogeneity length $L_{LS} = 2\pi q_{peak}^{-1}$, determined from the location of the peak observed in the light scattering data for samples B2B3(0.38) and B2B3(0.29) (Figure 6).

Phase Diagram. The free energy per segment for a mixture of two polymers can be approximated by[18]

$$\frac{F}{k_B T} = \frac{\Phi}{N_1}\ln\Phi + \frac{(1-\Phi)}{N_2}\ln(1-\Phi) + \chi\Phi(1-\Phi) \tag{14}$$

where k_B is the Boltzmann constant, χ is the Flory interaction parameter (see following section), and Φ and N are defined as in eq 1. We have computed the coexistence ($\partial F(\Phi')/\partial\Phi = \partial F(\Phi'')/\partial\Phi$) and stability ($\partial^2 F/\partial\Phi^2 = 0$) limits for mixtures B2B3(Φ) and B2B5(Φ) in terms of the degree of polymerization N_1 of the perdeuterated polymer B2

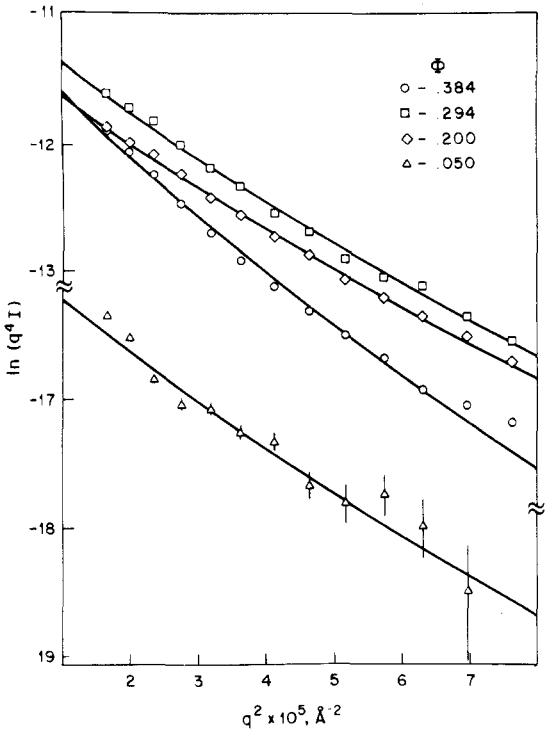

Figure 8. Porod plot of the SANS data (corrected for single chain scattering) obtained for the phase-separated mixtures (Figure 3). The curves correspond to the theoretical scattering function for a classical (mean-field) interfacial composition profile from which the interfacial thickness D and Porod heterogeneity length L_P have been determined.

(Table I), as presented in Figure 9. The conditions for stability and criticality ($\partial^2F/\partial\Phi^2 = \partial^3F/\partial\Phi^3$) can be expressed explicitly in terms of the product χN_1

$$(\chi N_1)_S = [\Phi^{-1} + (N_1/N_2)(1 - \Phi)^{-1}]/2 \quad (15)$$

$$\Phi_C = N_2^{1/2}/(N_1^{1/2} + N_2^{1/2}) \quad (16)$$

$$(\chi N_1)_C = (N_1^{1/2} + N_2^{1/2})^2/2N_2 \quad (17)$$

Comparison of the room temperature SANS results obtained from samples B2B5(0.31) and B2B5(0.65) (Figure 2) suggests that the interaction parameter does not depend strongly on composition. Therefore, we have assumed a single value of $\chi N_1 = 4.0$ for all of the mixtures investigated at $T = 296$ K. Sample locations in phase space have been assigned to Figure 9 accordingly.

Discussion

Overall, the results presented in the previous section conclusively demonstrate that mixtures of normal and perdeuterated 1,4-polybutadiene, otherwise of identical chemical structure, are characterized by an upper critical solution temperature (UCST); i.e., these mixtures *do not* form ideal solutions. As a consequence, increasing the molecular weight of the components induces composition fluctuations and subsequently phase separation as evidenced by the SANS results obtained from samples B2B5(Φ) and B2B3(Φ).

In the following discussions we focus on examining the underlying molecular origin of this documented isotope effect and consider the Porod scattering results, obtained from the phase-separated mixtures, in the context of current theories regarding polymer–polymer interfacial mixing.

Isotope Effect. Several years ago, Buckingham and Hentschel[27] predicted that mixtures of normal and deuterated high molecular weight polymers should exhibit

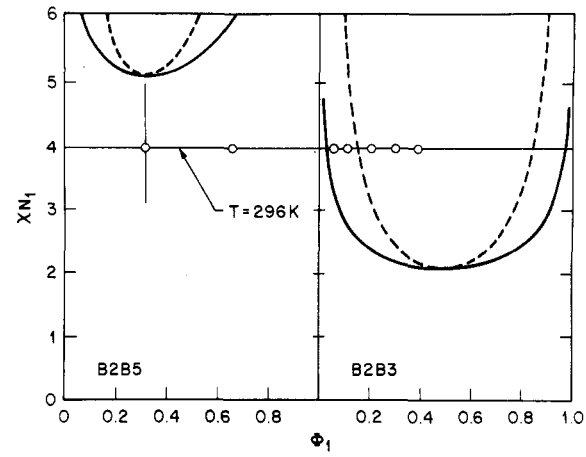

Figure 9. Phase diagram for mixtures B2B5(Φ) and B2B3(Φ) based on the Flory–Huggins approximation to the mixing free energy (eq 14), where N_1 and Φ represent the weight-average degree of polymerization and volume fraction of polymer B2, respectively. The solid and dashed curves correspond to the coexistence and stability limits. $\chi N_1 = 4.0$ at 296 K has been determined based on the SANS results obtained from the two homogeneous mixtures; this assumes that χ does not depend on composition.

segregation effects. These authors noted that all protonated and deuterated organic molecules are distinguished by slightly different molar volumes V, generally within the range $10^{-2} \leq \Delta V/V \leq 10^{-3}$ (analogous although considerably greater differences in the atomic volumes of ^{3}He and ^{4}He were speculated[28] long ago to be responsible for the low-temperature ($\simeq$0.9 K) UCST observed in liquid mixtures of these isotopes). In order to calculate the phase behavior of such mixtures, Buckingham and Hentschel (following Prigogine[28]) conceptually divided the mixing process into two steps: (i) compressing and dilating each pure component such that both polymer segment molar volumes equal that corresponding to the mixed state; (ii) mixing these components at constant volume, temperature, and pressure. Thus, the overall free energy of mixing is simply given by the sum of the change in free energy for each step, $\Delta F_{mix} = \Delta F^{(i)} + \Delta F^{(ii)}$. Buckingham and Hentschel estimate that interaction energy contributions to step ii are insignificant relative to the combinatorial entropy of mixing, so that $\Delta F^{(ii)}$ can be closely approximated by eq 14 with $\chi = 0$. $\Delta F^{(i)}$ is calculated based on classical thermodynamics[28] to be a function of composition, $\Delta V/V$, V, and isothermal compressibility κ. Assuming no excess volume of mixing ($V = \Phi_1V_1 + \Phi_2V_2$) and differentiating ΔF_{mix} with respect to composition, Buckingham and Hentschel have determined the phase diagram for mixtures of deuterated and protonated polymers. Owing to the definition of $\Delta F^{(ii)}$, this phase diagram resembles that presented in Figure 9, except that it is explicit in temperature rather than χ, specifically predicting an upper critical solution temperature (UCST), *in qualitative agreement with our results*. This theory can be quantitatively evaluated by comparing the predicted critical point for a given composition with that corresponding to the experimentally determined value of χ. For simplicity, we consider the symmetrical case ($N = N_1 = N_2$; $\Phi_1 = \Phi_2 = 0.5$) for which Buckingham and Hentschel predict

$$N_C = 4k_BT\kappa/V(\Delta V/V)^2 \quad (18)$$

For normal and perdeuterated 1,4-polybutadiene, $\kappa = 5.3 \times 10^{-10}$ Pa^{-1},[19] $V = 1.00 \times 10^{-22}$ cm^3, and $\Delta V/V = 4.1 \times 10^{-3}$. Therefore at 296 K the predicted critical degree of polymerization is $N_C = 5.2 \times 10^3$. This result can be compared with the SANS-determined χ parameter by

using the symmetrical version of eq 17, $N_C = 2/\chi$. Based on the interaction parameter corresponding to 296 K (Figure 7), the experimentally determined value is $N_C = 2.3 \pm 0.5 \times 10^3$. Thus, this simple theory identifies the qualitative nature of the observed isotope effect in *both* high molecular weight polymers and helium. (Since submitting this paper we have quantitatively identified the nature of the isotope effect as described in ref 35.)

It should be noted that the above-described theory is a special case of the equation-of-state theory presented by Flory[29] over two decades ago. In general, equation-of-state contributions to the free energy of mixing are manifested as a lower critical solution temperature (LCST) and a composition-dependent interaction parameter; both of these effects derive from differences in component thermal expansivity, compressibility, and "contact agility".[30] In the present case these physical differences are negligible; the only significant difference is in segment volumes.

Interfacial Mixing. Helfand et al.[23] provided the first description of interfacial mixing in phase-separated polymer mixtures. In the limit of strong incompatibility $\chi N \gg (\chi N)_S$ the composition profile across a phase boundary is given by eq 11, where the characteristic length depends on the magnitude of the interaction parameter

$$D = a/(6\chi)^{1/2} \tag{19}$$

Until present, interfacial thickness measurements have been restricted to this narrow interface regime, $D \sim 10$ Å,[31,32] whereby sufficient Porod scattering intensity is obtained by examining microphase-separated block copolymers characterized by large surface-to-volume ratios.

More recently, Leibler[24] has developed a mean-field formalism describing polymer–polymer interfaces for mixtures lying near the consolute point. This approximate theory also predicts a classical (mean-field) interfacial profile as given by eq 11, except that the characteristic length now depends on the relative distance of a sample from the critical point. For the symmetric case ($N_1 = N_2 = N$)

$$D = a/[(9/2)(\chi - 2/N)]^{1/2} \tag{20}$$

so that the interfacial thickness is predicted to diverge at the consolute point. In the limit $N \to \infty$, this expression reduces to the exact *form* (eq 19) differing only by a factor of $(4/3)^{1/2}$. This discrepancy most likely derives from neglecting higher order terms in the free energy expansion; i.e., eq 20 is applicable as $\chi N \to (\chi N)_C$.

The Porod scattering results presented in Figure 8 provide quantitative information regarding three distinct aspects of interfacial mixing in phase-separated polymer blends: (1) the form indicates the composition *profile* of the interface, (2) the slope establishes interfacial *thickness*, and (3) the absolute level (intercept) provides a measure of the total *surface* area of a sample. We initially consider each of these features separately.

For $qD \geq 1$, the form of the Porod scattering from a two-phase mixture becomes sensitive to the detailed structure of the interface as illustrated in Figure 10. The linear and sigmoidal models referred to in Figure 10 have been previously discussed by Vonk[33] and Hashimoto et al.[32] respectively, while the classical form corresponds to that given by eq 11. It is evident that the observed intensity in this scattering regime is quite sensitive to the level of mixing in the "wings" of the interfacial profile. Within experimental error, the SANS results presented in Figure 8 discriminate in favor of the theoretically derived interfacial composition profile (eq 11) as demonstrated by the solid curves.

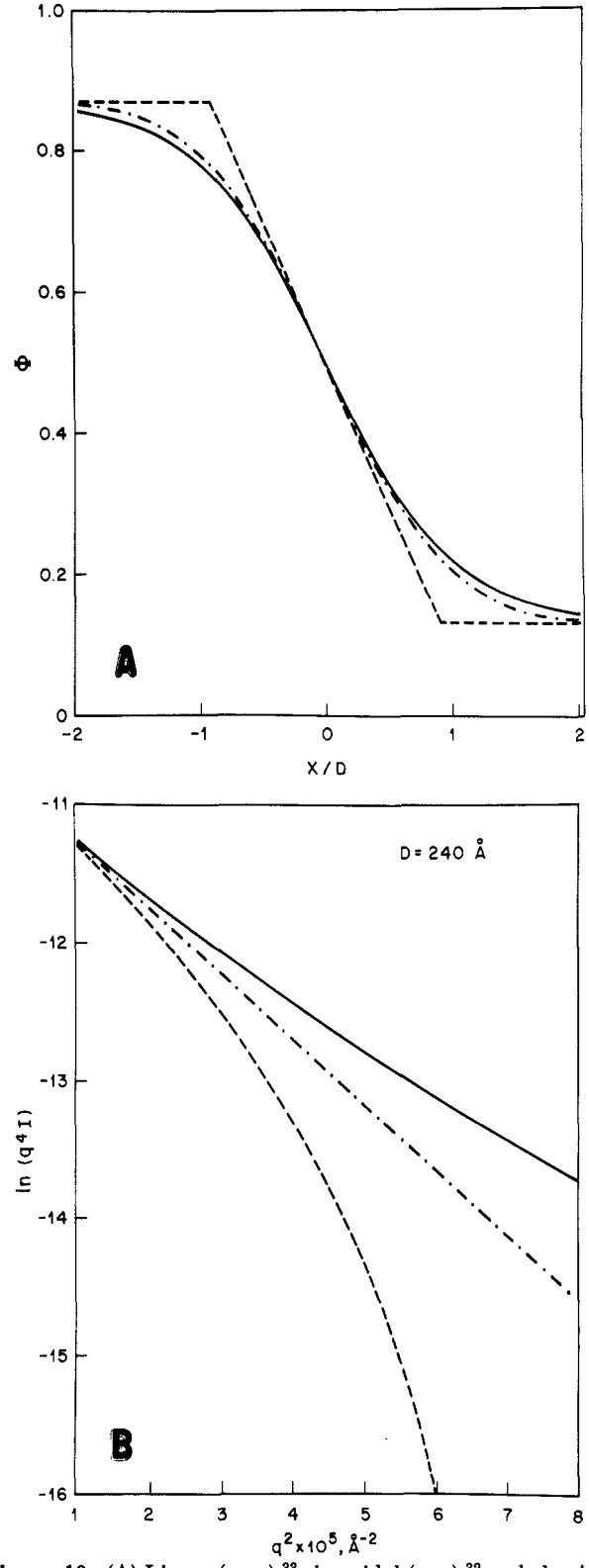

Figure 10. (A) Linear (– – –),[33] sigmoidal (– · –),[32] and classical (—) (eq 11) interfacial composition profiles between symmetric polymers expressed in units of interfacial thickness D. (B) Theoretical small-angle (Porod) scattering (eq 9 and 12) corresponding to the illustrated composition profiles. In the limit $Dq \ll 1$ these scattering patterns are indistinguishable.

The phase-separated mixtures are characterized by essentially a single interfacial thickness (Table II) $\langle D \rangle = 250$ Å, which is more than 25 times greater than that previously reported for poly(styrene–diene) block copolymers.[31,32] On the basis of the interaction parameter (assumed to be composition independent) determined in the homogeneous state (Figure 7) and by the neglect of small difference in

degree of polymerization between polymers B2 and B3 ($\langle N \rangle$ = 4400), the predicted interfacial thickness (eq 20) is calculated to be D = 160 Å. In light of the approximate form of the theory and the assumption that χ does not depend on Φ, the calculated and experimental results are in reasonable agreement.

The measured Porod heterogeneity lengths L_P listed in Table II fall into two distinct categories: $L_P \cong 0.3$ μm (Φ = 0.38, 0.29, 0.20) and $L_P \cong 35$ μm (Φ = 0.10, 0.05). This is consistent with the relative locations of these samples in phase space (Figure 9). Mixtures situated above the stability limit (dashed curve) are expected to spontaneously demix (spinodal decomposition) upon the removal of solvent, producing a fine-grain heterogeneous morphology,[21] while mixtures located within the metastable gap, between the coexistence (solid curve) and stability limits should demix via a nucleation process, leading to a considerably coarser two-phase structure.[21]

Finally, the heterogeneity length, L_{LS} (Table II), determined by light scattering (Figure 6) is approximately 15 times that obtained from the Porod analysis of the SANS data Figures 3 and 8). L_{LS} is expected to be several times larger than L_P since the former represents a "weight-average" length, determined by the average distance between domains, while the latter corresponds to the total sample volume-to-surface ratio, regardless of domain size distribution.[4] Furthermore, L_P has been calculated based on the assumption of an ideal periodic structure (eq 10); a spherical or convoluted morphology would lead to a several-fold underestimation of L_P relative to L_{LS}. The two-phase structures are thus most likely *both* highly disperse *and* convoluted in structure. This is consistent with the preparation history of these mixtures (solvent casting) and the probably spinodal decomposition process of demixing.

Conclusions

We have conclusively demonstrated by means of small-angle neutron scattering (SANS) measurements that binary liquid mixtures of perdeuterated and normal 1,4-polybutadienes are characterized by an upper critical solution temperature (UCST) in contradiction with the typical assumption of ideal solution behavior; we have also recently demonstrated this effect in mixtures of perdeuterated and normal polystyrenes.[34] This phenomenon, which is quantitatively predicted by Buckingham and Hentschel,[27] derives from a small measurable difference in segment volume between normal and deuterated polymers. Increasing molecular weight above the critical value produces phase separation, accompanied by extensive interfacial mixing over distances comparable to the size of the polymeric constituents. The interfacial composition profile has been determined by SANS to be in qualitative agreement with the mean-field theory of Leibler.[24]

These findings clearly indicate that the isotope labeling technique must be employed with caution. However, it can also be concluded that normal and deuterium-labeled polymers represent an exciting new class of mixtures with which to study high molecular weight polymer–polymer phase behavior.

Acknowledgment. P. J. Carroll provided technical assistance in the light scattering measurements. We are grateful to Dr. E. Helfand and Dr. W. C. Koehler for helpful suggestions and for many stimulating discussions of this work.

Research at the National Center for Small Angle Scattering Research, Oak Ridge National Laboratory was sponsored by the National Science Foundation under Grant DMR-7724459, with the U.S. Department of Energy under Contract DE-AC05-840R21400 with Martin Marietta Energy Systems, Inc.

Registry No. 1,4-Polybutadiene, 9003-17-2; perdeuterated 1,4-polybutadiene, 29989-19-3.

References and Notes

(1) Kirste, R. G.; Kruse, W.; Schelten, J. *Makromol. Chem.* **1972**, *162*, 299. Benoit, M.; Cotton, J. P.; Decker, D.; Farnoux, B.; Higgins, J. S.; Jannink, G.; Ober, R.; Picot, C. *Nature (London)* **1973**, *245*, 13.
(2) Wignall, G. D.; Ballard, D. G. H.; Schelten, J. *Eur. Polym. J.* **1973**, *9*, 965. Wignall, G. D.; Ballard, D. G. H.; Schelten, J. *Eur. Polym. J.* **1974**, *10*, 861.
(3) Wignall, G. D. *Encycl. Polym. Sci.*, in press.
(4) Glatter, O., Kratky, O., Eds. *Small Angle X-Ray Scattering*; Academic: London, 1982.
(5) *Handbook of Chemistry and Physics*, 56th ed.; CRC Press: Boca Raton, FL, 1975.
(6) Stehling, F. C.; Ergos, E.; Mandelkern, L. *Macromolecules* **1971**, *4*, 672.
(7) Schelten, J.; Wignall, G. D.; Ballard, D. G. H. *Polymer* **1977**, *18*, 1111.
(8) Strazielle, C.; Benoit, H. *Macromolecules* **1975**, *8*, 203.
(9) Atkin, E. L.; Kleinjens, L. A.; Koningsveld, R.; Fetters, L. J. *Makromol. Chem.* **1984**, *185*, 377.
(10) Yang, H.; Hadziioannou, G.; Stein, R. S. *J. Polym. Sci., Polym. Phys. Ed.* **1983**, *21*, 159.
(11) The critical temperature for mixtures of 2,6-lutadiene and water changes by ~1 °C if heavy water is substituted for normal water: Huang, J. S., personal communication.
(12) Wilks, J. *Properties of Liquid and Solid Helium*; Oxford University Press: Oxford, 1967.
(13) Bates, F. S.; Wignall, G. D.; Koehler, W. C. *Phys. Rev. Lett.* **1985**, *55*, 2425.
(14) Clague, A. D. H.; Vanbroek, J. A.; Blaauw, L. P. *Macromolecules* **1974**, *7*, 348.
(15) Bates, F. S.; Bair, H. E.; Hartney, M. A. *Macromolecules* **1984**, *17*, 1987.
(16) ASTM No. D792, *Annual Book of ASTM Standards*; American Society for Testing and Materials: Philadelphia, 1983; Vol. 8.01.
(17) Bartell, L. S.; Roskos, R. R. *J. Chem. Phys.* **1966**, *44*, 457.
(18) de Gennes, P.-G. *Scaling Concepts in Polymer Physics*; Cornell University Press: Ithaca, NY, 1979.
(19) Bacon, G. E. *Neutron Diffraction*, 3rd ed.; Oxford University Press: London, 1975.
(20) Brandrup, J., Immergut, E. H., Eds. *Polymer Handbook*; Wiley: New York, 1975.
(21) Binder, K. *J. Chem. Phys.* **1983**, *79*, 6387.
(22) Ruland, W. *J. Appl. Crystallogr.* **1971**, *4*, 70.
(23) Helfand, E.; Tagami, Y. *J. Chem. Phys.* **1971**, *56*, 3592. Helfand, E.; Sapse, A. M. *J. Chem. Phys.* **1975**, *62*, 1327.
(24) Leibler, L. *Macromolecules* **1982**, *15*, 1283.
(25) Cahn, J. W.; Hilliard, J. E. *J. Chem. Phys.* **1958**, *28*, 258.
(26) Helfand, E.; Wasserman, Z. R. In *Developments in Block Copolymers*; Goodman, I., Ed.; Applied Science: London, 1982.
(27) Buckingham, A. D.; Hentschel, H. G. E. *J. Polym. Sci., Polym. Phys. Ed.* **1980**, *18*, 853.
(28) Prigogine, I. *The Molecular Theory of Solutions*; North-Holland: Amsterdam, 1957.
(29) Flory, P. J. *J. Am. Chem. Soc.* **1965**, *87*, 1833.
(30) Liu, D. D.; Prausnitz, J. M. *Macromolecules* **1979**, *12*, 454.
(31) Bates, F. S.; Berney, C. V.; Cohen, R. E. *Macromolecules* **1983**, *16*, 1101.
(32) Hashimoto, T.; Shibayama, M.; Kawai, H. *Macromolecules* **1980**, *13*, 1237. Hashimoto, T.; Fujimura, M.; Kawai, H. *Ibid.* **1980**, *13*, 1660.
(33) Vonk, C. G. *J. Appl. Crystallogr.* **1973**, *6*, 81.
(34) Bates, F. S.; Wignall, G. D. *Macromolecules* **1986**, *19*, 932.
(35) Bates, F. S.; Wignall, G. D. *Phys. Rev. Lett.*, submitted.